Environmental Advances 7 (2022) 100167

Contents lists available at ScienceDirect

Environmental Advances

journal homepage: www.sciencedirect.com/journal/environmental-advances

Characterization of relevant site-specific PFAS fate and transport processes at multiple AFFF sites

David T. Adamson [a,*], Poonam R. Kulkarni [a], Anastasia Nickerson [b], Christopher P. Higgins [b], Jennifer Field [c], Trever Schwichtenberg [c], Charles Newell [a], John J. Kornuc [d]

[a] GSI Environmental Inc., 2211 Norfolk Suite 1000, Houston, TX 77098, United States
[b] Department of Civil and Environmental Engineering, Colorado School of Mines, 1500 Illinois St, Golden, CO 80401, United States
[c] Department of Environmental and Molecular Toxicology, Oregon State University, Corvallis, OR 97331, United States
[d] Naval Facilities Engineering and Expeditionary Warfare Center, 1100 23rd Avenue, Port Hueneme, CA 93041, United States

ARTICLE INFO

Keywords:
PFAS
AFFF
Groundwater
Natural attenuation
Remediation

ABSTRACT

The relevance of multiple poly- and perfluoroalkyl substance (PFAS) fate and transport process across multiple sites was established through high-resolution characterization of the spatial distribution of PFAS within aqueous film forming foam (AFFF)-related source areas and the downgradient plumes. The maximum total PFAS concentrations in source area groundwater at the three study sites ranged from 6 to 51 mg/L but consistently decreased by several orders of magnitude with distance from the source area at all sites, indicating that non-destructive attenuation of PFAS occurred along each flow path. The relative distribution of different PFAS classes, including zwitterionic/cationic species, provided site-specific lines of evidence for retardation due to hydrophobic, air-water interfacial, and electrostatic partitioning processes, as well as impacts from biotransformation and matrix diffusion at multiple sites. The only site where one of these processes (air-water interfacial partitioning) was not supported by the data (Site 1) was attributable to disturbance of vadose zone soils as part of historic remedial efforts. In other cases, the magnitude that these processes influenced PFAS transport reflected site-specific conditions. This included apparent salting out of PFAS at Site 2 due to its elevated groundwater salinity, which has implications for plume migration in coastal areas. In addition, PFAS was present in lower-permeability soils at each site, suggesting that longer-term retention of PFAS is occurring in these zones. The finding that multiple processes were active at site-wide scales is consistent with expectations that these are naturally occurring reactions that should be relevant at most AFFF-impacted source zones.

Introduction

The release of products or wastes containing poly- and perfluoroalkyl substances (PFAS) has led to their widespread occurrence in a variety of environmental media (Rankin et al., 2016; Anderson et al., 2016; Hatton et al., 2018; Brusseau et al., 2020). A particular concern has been the potential for PFAS in aqueous film-forming foam (AFFF) to enter groundwater and pose a risk to drinking water supplies (Guelfo and Adamson, 2018; Leeson et al., 2021). AFFF is generally released as part of fire response or fire training activities within specific areas, where they can serve as a potential long-term source of PFAS. Because PFAS are not expected to naturally degrade beyond the perfluoroalkyl acids (PFAAs), there is a concern that remediation of AFFF-related PFAS source areas will be necessary at many sites. Significant characterization of the PFAS sources and distribution at an individual site is a prerequisite to making informed remedial decisions, and documenting the fate and transport processes that have contributed to the observed distribution is a clear priority for building the conceptual site model.

Recent lab-scale and field-scale research has increased our understanding of physical, chemical, and biological processes that are potentially relevant to PFAS migration at AFFF sites (Guelfo et al., 2021). This includes extensive studies that document the importance of partitioning of certain PFAS to the air-water interface in unsaturated porous media (Costanza et al., 2019; Schaefer et al., 2019; Costanza et al., 2020; Lyu and Brusseau, 2020; Silva et al., 2021; Sharifan et al., 2021), which is expected to be a function of both solution chemistry and PFAS properties. Within saturated systems that mimic aquifer conditions, partitioning of PFAS to solid phases through hydrophobic

* Corresponding author.
E-mail address: dtadamson@gsi-net.com (D.T. Adamson).

https://doi.org/10.1016/j.envadv.2022.100167
Received 4 January 2022; Accepted 7 January 2022
Available online 13 January 2022

(nonionic) sorption and electrostatic interactions are recognized mechanisms for PFAS retention (Higgins and Luthy, 2006 2006; Du et al., 2014; Guelfo and Higgins, 2013). In groundwater, these would be expected to retard the transport rates of certain PFAS with higher affinity to organic carbon (e.g., more hydrophobic, longer-chain PFAS) and/or charge distributions that enhance attraction to soil particles (e.g., PFAS with zwitterionic/cationic functional groups) (Barzen-Hanson et al., 2017; Xiao et al., 2019; Mejia-Avendano, 2020; Nguyen et al., 2020). Lab-based studies have documented that several of these processes are enhanced when the ionic strength of the aqueous phase is increased (Costanza et al., 2019; Lyu and Brusseau, 2020), along with "salting out" of PFAS in high-salinity water environments where the PFAS become increasingly associated with the solid phase (Munoz et al., 2017; Wang et al., 2020; Newell et al., 2021). Other in situ processes such as biotransformation of polyfluorinated precursors and diffusion of PFAS into lower permeability zones that are poorly flushed by advection (Adamson et al., 2020) may also be relevant at many AFFF-impacted sites.

Collectively, these fate and transport processes may lead to different spatial distributions of PFAS when compared to compounds that are subject to destructive attenuation. At sites where a strong source is providing a consistent input of a non-attenuating compound to groundwater, a constant-concentration front would be expected to extend downgradient from the source. While there are limited data suggesting that PFAS behave differently once released to the subsurface (Adamson et al., 2020), it is not clear if the processes that contribute to attenuation of PFAS with distance are ubiquitous or highly site-specific. Anderson et al. (2019) presented empirical evidence using data aggregated across 40 sites to show that PFAS properties (including chain length) influenced the soil-to-water ratios observed in samples from those sites. These data suggest that the mechanisms that contribute to differential transport of individual PFAS may be relevant across AFFF sites. Increasingly, field-scale PFAS characterization efforts have been aided by applying high-resolution sample and data acquisition protocols (McGuire et al., 2014; Baudel et al., 2017; Dauchy et al., 2019; Høisæter et al., 2019; Quinnan et al., 2021) that can provide robust data to establish PFAS distribution. In addition, efforts to quantify all PFAS that might be present at AFFF-impacted sites have been enhanced by the continued progression of non-target and high-resolution analyses that can identify a much larger suite of PFAS than conventional methods, including zwitterionic and cationic compounds (Liu et al., 2019; McDonough et al., 2019; Nickerson et al., 2020a; Sorengard et al., 2020).

This study hypothesized that specific processes that might be expected to influence PFAS fate and transport are widely relevant at actual AFFF-impacted sites for several reasons. First, the nature of AFFF products and usage means that PFAS are released as a complex mixture of compounds that have wide-ranging transport properties that lends itself to differential transport. Second, AFFF is released at the ground surface, such that PFAS must interact with the vadose zone compartment where air-water interfacial partitioning processes may dampen the PFAS mass that discharges to deeper intervals and ultimately migrates in groundwater. Third, these processes occur naturally and rely on commonly encountered site characteristics (e.g., the presence of natural organic carbon, neutral pH), as opposed to niche or highly engineered conditions (e.g., the presence of specific mineral species, substrates, or microbes) (Weber et al., 2017). The objective of this study was to perform high-resolution characterization of multiple AFFF-impacted sites to better understand the prevalence of these suspected PFAS fate and transport processes and establish how they influence PFAS distribution on site-wide scales. This expands upon previous evaluations of one of these sites (Nickerson et al., 2020b; Adamson et al., 2020; Site 1 here) that showed that a significant portion of the remaining PFAS mass, particularly precursors, was still located near the source, while biotransformation and other processes were contributing to trends within the plume. In this study, the relevance of multiple non-destructive processes on PFAS distribution was documented at each site, which has implications for predicting PFAS behavior over time and ultimately how to manage these sites to reduce risk.

Methods and materials

Site locations

Field data were collected at three different U.S. military bases where AFFF was used for firefighting support. Site 1 is located in the southeastern U.S. and consisted of a firefighting training area where a shallow unlined pit was used for training activities between 1968 and 1991. A full description of Site 1 is included in Nickerson et al. (2020b). Site 2 is a coastal facility with tidal influences located on the west coast of the U.S. and occupies an open area that includes two co-located fire training pits: one closed and one active. The closed burn pit was used for firefighter training from the late 1950s to 1984. Even though the active burn pit is available for use as a fire training area, exercises involving AFFF reportedly ceased in the mid-2000s. Site 3 is an inland site located near the east coast of the U.S. where AFFF was used historically during firefighting activities and emergencies. The study area of Site 3 was an AFFF storage and transfer area.

Data collection

A similar protocol for collecting depth-discrete soil and groundwater samples was followed at each site. Multiple locations were characterized at each site with the focus on source areas, several downgradient locations, and a minimum of one upgradient (background) location (Figure 1). Data were generally collected along one transect that followed the groundwater flow direction, as well as two or more cross-gradient transects. Subsurface samples were obtained using a direct push rig (Geoprobe Model 6620DT) that collected soil cores (4.7-cm diameter, 1.5-m length) and groundwater from co-located boreholes (< 0.5 m apart). Groundwater samples were collected from at least four depths at all investigation points using a combination of exposed screen sampling (0.6-m length) during advancement of casing with the rig and/or temporary piezometers installed at targeted depths. At some sites, existing monitoring wells were sampled. Soil sampling locations were chosen to coincide with groundwater sampling locations, and multiple subsamples were collected from each core. Surface soil samples were also collected at each location, as well as additional locations where groundwater and subsurface soil sampling were not completed. The Hydraulic Profiling Tool (Geoprobe) was used to provide stratigraphic information in combination with visual inspection and logging of soil cores. Samples were collected in matrix-specific containers and shipped to analytical labs for further processing based on lab-specific protocols (Nickerson et al., 2020a). Not including samples for quality assurance/quality control purposes, a total of 58 depth-discrete groundwater samples and 105 depth-discrete soil samples were collected from Site 1; 38 groundwater and 72 soil samples were collected from Site 2; and 49 groundwater and 87 soil samples were collected from Site 3.

PFAS analysis was completed using matrix-specific techniques that are described in detail in Nickerson et al. (2020a; 2020b) and Schwichtenberg et al. (2020). Soil samples were dried and homogenized before spiking with 4 ng of all isotopically labeled standards. Extraction followed the method described in Nickerson et al (2020a) where two rounds of basic methanol (0.1 M ammonium hydroxide in methanol) and two rounds of acidic methanol (0.5 M hydrochloric acid in methanol) were used as solvents. This was followed by solid-phase extraction (using ENVI-Carb) for cleanup, neutralization, evaporation, and reconstitution. Soil data from all sites were acquired using LC-QTOF-MS. Target analytes consisted of compounds for which an analytical standard was available, while suspect hits from LC-QTOF-MS were defined as those without analytical standards but meeting specified criteria as described previously (Nickerson et al., 2020a). Groundwater samples

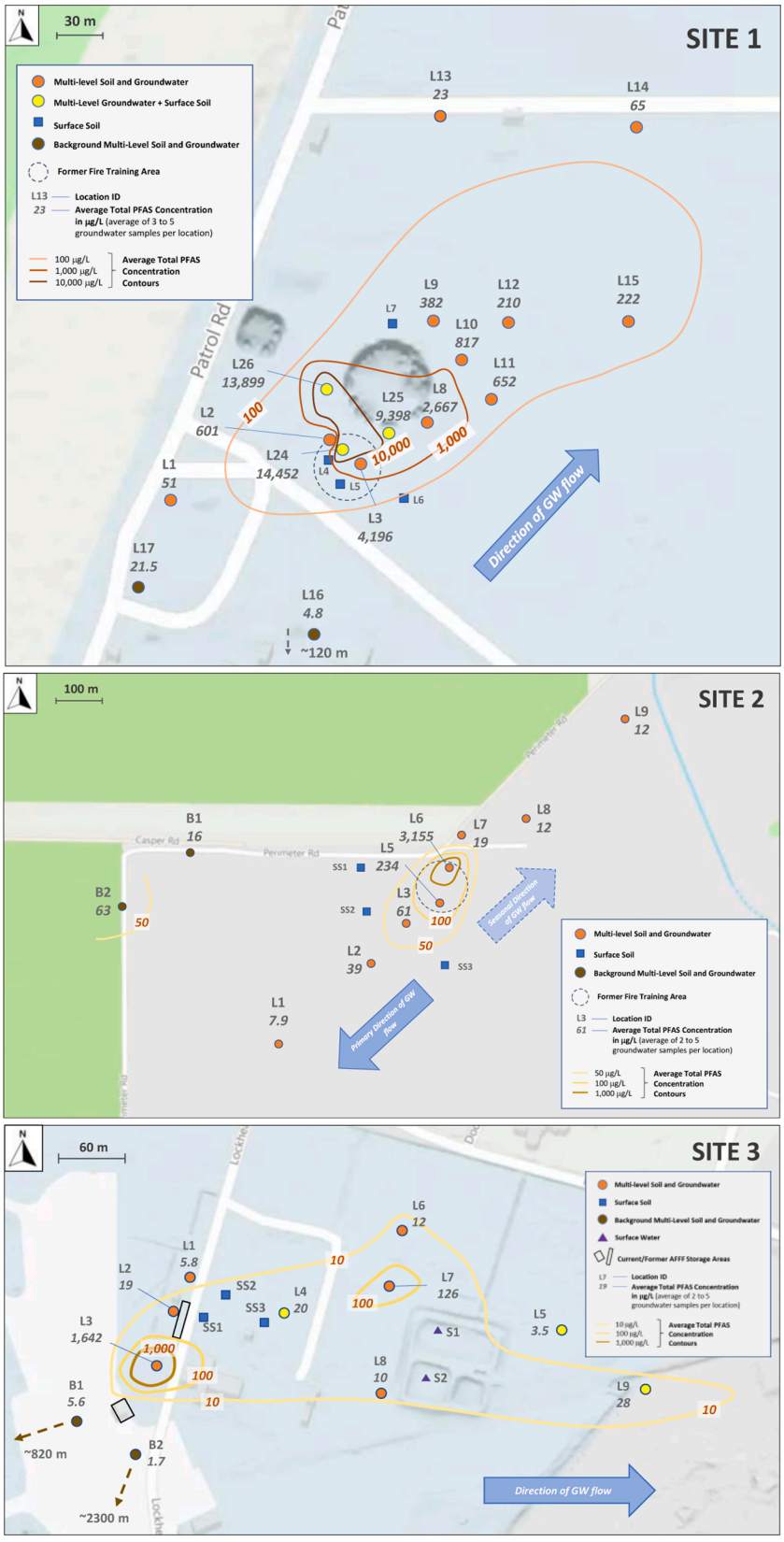

Fig. 1. Average Concentration of Total PFAS in Groundwater Samples from Site 1 (top panel), Site 2 (middle panel), and Site 3 (bottom panel). Values represent the average total PFAS concentration in groundwater samples from the designated site locations (µg/L). Three to five depth-discrete concentrations from each contributing location were averaged to generate a concentration for those datapoints. Contours are approximate. See Supporting Information for contours of surface soil and saturated soil PFAS data for each site.

from Site 1 went through multiple rounds of extraction d using a liquid-liquid extraction procedure involving sodium chloride, hydrochloric acid (6 M), and isotopically labeled standards, along with a solvent (1 mL) comprised of 90:10 ethyl acetate:2,2,2-trifluoroethanol. Diluted extracts were analyzed using LC-MS/MS protocols described in Nickerson et al. (2020b), while groundwater from Site 2 and Site 3 were analyzed by LC-QTOF-MS to permit screening and semi-quantitation of a larger number of non-target analytes. Initial sample preparation steps

for groundwater analysis included the addition of sodium chloride and HCl to 6 mL of the sample followed by spiking with 1.5 ng of 30 isotopically labeled surrogate standards. Water was extracted three times with ethyl acetate and trifluoro ethanol; the final extract was spiked with 0.75 ng of M2PFOA and M8PFOS. No positive mode surrogates were spiked into samples.

Data from each location were compiled using modified designations described in Nickerson et al (2020). Major groupings included PFAAs (perfluorinated carboxylates and perfluorinated sulfonates) potential precursors (all non-PFAAs), anionic PFAS (which included PFAAs and target and suspect non-PFAAs identified using LC-QTOF-MS in electrospray ionization negative mode, and zwitterionic/cationic PFAS (which included target and suspect cationic/zwitterionic non-PFAAs identified using LC-QTOF-MS in electrospray ionization positive mode).

Hydrogeology

At each site, characterization focused on the shallowest groundwater bearing unit within unconsolidated formations. Representative cross sections are shown in Figure S1 – S3. Total depths of investigation points ranged from 10.7 to 15.2 m below ground surface (bgs) at Site 1, 7.6 to 15.2 m at Site 2, and 9.1 to 13.4 m bgs at Site 3. The depth to water was < 1.8 m bgs at Site 1 and Site 2, and between 1.2 to 2.1 m bgs at Site 3 depending on location. Groundwater flow directions and seepage velocities were estimated based on static water level data obtained during current and/or previous investigations. At each site, permeable intervals consisting largely of poorly-graded sands were encountered, but zones with contrasting permeabilities were also identified, including: (i) two clay/silt layers, along with significant silty sands, that underly the more permeable intervals at Site 1; (ii) lower-permeability clay and silt lenses at shallow depths at Site 2, with increasing thickness toward the northeast portion of the site; and (iii) a thin but laterally extensive lower-permeability clay and silt layer within the first 1.5 m at Site 3, along with a silt and clay confining layer approximately 1.5 to 3.0 m thick that separates the overlying aquifer from a deeper coarse sand unit. Cross-sections of representative transects from each site are shown in Figures S1 – S3.

Results and discussion

Identification of source areas

Representative PFAS contour maps for each site are shown in Figure 1 (total PFAS concentration in groundwater) and Figures S4 – S9 (soil concentration data). At all three sites, the highest total PFAS concentrations in both soil and groundwater were found in samples collected in the immediate vicinity of the former fire training area (Site 1 and Site 2) or AFFF storage and transfer area (Site 3) (Table 1). A similar pattern was observed for most individual PFAS. In addition, the highest PFAS concentrations in surficial soils were observed within the same general area. These distributions supported the assumption that AFFF used in the vicinity of these identified areas is the primary source of PFAS in the subsurface. One difference was noted at Site 3, where the near surface soil concentrations at two mid-plume locations (L7 and L8) were consistently higher than those at several locations (L1, L3, SS1, SS2, and SS3) that are all much closer to the presumed source area. Given that PFAS surficial soil concentrations are also higher than those at deeper intervals at these mid-plume locations, these data suggests that runoff and/or usage of AFFF may have occurred in areas beyond the expected release areas at Site 3.

Electrochemical fluorination (ECF)-based AFFF was expected to have been used at each site. This was confirmed based on the high concentration of PFOS as well as the widespread occurrence of PFOS at expected branching percentage (i.e., percent of branched PFOS isomer) in groundwater (approximately 30%) (Benskin et al., 2010). Telomer-based AFFF was also presumably used at each site, as evidenced by the presence of elevated levels of multiple fluorotelomers within the source area (e.g., 4:2 FTS, 6:2 FTS, 8:2 FTS) and several PFOA groundwater samples where the branching percentage was lower than expected for PFOA in ECF-based foams (Table S1).

Downgradient concentration trends

PFAS migration from the source area was confirmed at all three sites by the presence of measurable levels of PFAS in all groundwater samples, including those from the farthest downgradient locations that ranged from 280 to 530 m per site. Given the mobility of some PFAS and the decades-old timescale of releases, plume development should be expected. However, concentrations of PFAS in groundwater rapidly decreased with distance from the source area at all sites, typically by two to three orders of magnitude (Figure 2). This was further illustrated for Site 1 by estimation of mass discharge rates that decreased by 99% from the source area to the downgradient transect (Adamson et al., 2020). This pattern suggests that non-destructive attenuation of PFAS is occurring along the flow path at these sites, as opposed to a more uniform concentration vs. distance profile that would represent a non-attenuating strong source. As described below, the spatial distribution of PFAS along the downgradient groundwater flow path at these three sites, including compositional changes, suggests that one or more processes were actively affecting PFAS transport.

Hydrophobic, electrostatic, and salinity-enhanced partitioning

The distribution of different PFAS moving downgradient of the source areas was used to investigate the role of solid-phase adsorption. For example, precursors generally represented a lower percentage of the total PFAS concentration with distance downgradient of the source at Site 1 (Adamson et al., 2020) (Figure S10 - S11). Specifically, zwitterionic/cationic PFAS are located primarily within the source area. This pattern suggests that these precursor compounds are migrating slower than anionic PFAS due to enhanced electrostatic attraction to largely negatively charged aquifer solid surfaces and potential biotransformation (Figure S10 - S11). In addition, the carbon chain length of PFAS in groundwater samples from the source area and nearby vicinity

Table 1
Maximum concentration of different PFAS categories by site.

Site Number	Total PFAS		Total PFAA [a]		Total Zwitterionic/ Cationic PFAS	
	Soil (ng/g)	Ground-water (ng/L)	Soil (ng/g)	Ground-water (ng/L)	Soil (ng/g)	Groundwater (ng/L)
Site 1	30,000	51,400,000	4,100	30,900,000	29,000	1,360,000
	(L3; 4.0 m)	(L24; 3.0 m)	(L24; 0.8 m)	(L26; 3 m)	(L3; 4.0 m)	(L24; 1.5 m)
Site 2	13,400	6,000,000	12,100	4,550,000	1,930	81
	(L6; 2.1 m)	(L6; 3.7 m)	(L6; 2.1 m)	(L6; 3.7 m)	(L5; 0.3 m)	(L8; 5.8 m)
Site 3	9,580	6,510,000	2,120	4,430,000	6,300	6,190
	(L3; 0.3 m)	(L3; 1.8 m)	(L3; 0.3 m)	(L3; 1.8 m)	(L3; 0.3 m)	(L3; 1.7 m)

Note: Values represent the maximum media-specific concentrations observed in any sample collected at each site along with the specific location (see Figure 1 for location details) and depth below ground surface (in m).

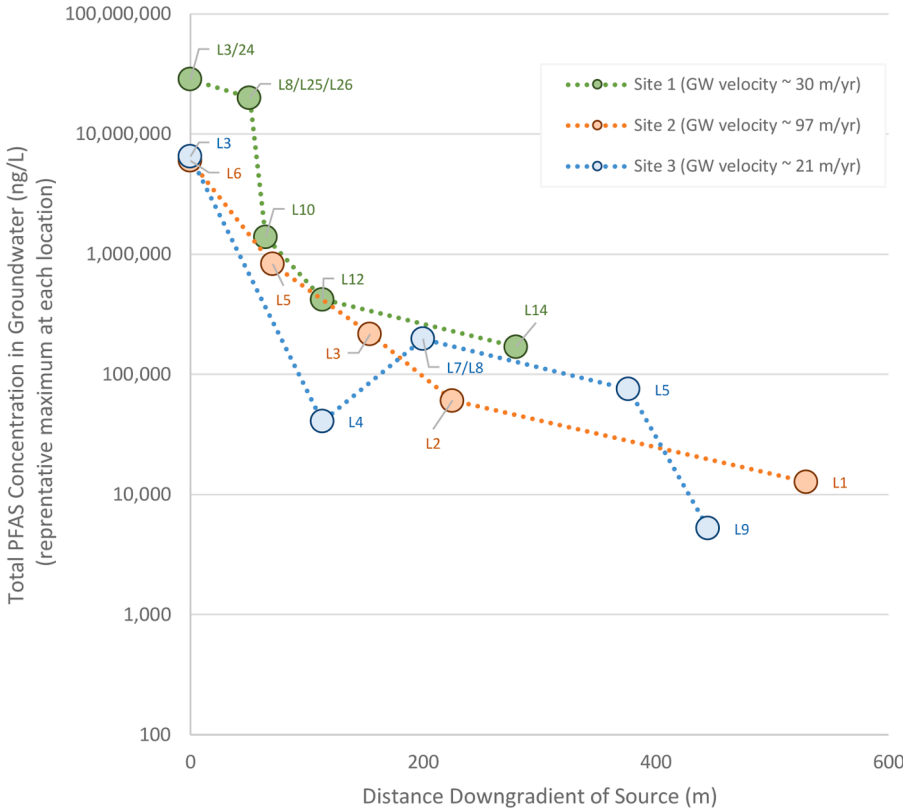

Fig. 2. Trends in Total PFAS Concentration in Groundwater with Distance Downgradient of Sources for Each Site. Each datapoint represents the maximum total PFAS concentration in samples from the designated site locations. Several datapoints represent multiple locations within a cross-gradient transect; the maximum concentrations from each contributing location were averaged to generate a representative maximum concentration for those datapoints.

(6.05–6.74) is generally higher than in groundwater samples located near downgradient (5.82–6.75) and far downgradient (5.83–6.43) (Figure S12). However, the general spatial trend is consistent with preferential hydrophobic partitioning of longer-chain PFAS and less retardation of shorter-chain PFAS during groundwater transport. When only PFCAs were considered, the carbon chain lengths in samples from the source area (0.60-1.55) tended to be shorter than those in the near downgradient (0.63-1.91) and far downgradient (1.96-3.87) areas, with the latter being significantly different than was observed in the source area (two-sided Wilcoxon Rank Sum test; p=0.003).

At Site 2, there was a similar decrease in the representative carbon chain length moving away from the source (Figure S15). In addition, the concentrations of zwitterionic/cationic species in groundwater were low outside of the source area at Site 2, as were their contribution to the total PFAS measured in groundwater (median of all samples = 1%; maximum of all samples = 24%) (Figure S14 - S15). At Site 3, zwitterionic/cationic PFAS also generally represented a low percentage of the total PFAS in groundwater (median of all samples = 2%; maximum of all samples = 49%) (Figure S16 - S17), and higher concentrations of zwitterionic/cationic PFAS were measured in the soil samples from the source area relative to those measured in downgradient locations. Several shallow samples from location L3 at Site 3 had zwitterionic/cationic PFAS concentrations greater than 1,000,000 ng/kg that represented a relatively high percentage of the total PFAS (> 40%). However, zwitterionic/cationic PFAS also represented a high percentage of the total PFAS in shallow soil samples in several downgradient locations at Site 3 (albeit at low concentrations), suggesting that source material was released and retained outside of the primary footprint of the AFFF storage/transfer area. This also may have influenced the PFAS chain length distribution at Site 3, which followed the expected pattern (i.e., decreasing chain length with distance from the source) (Figure S18).

In addition, the naturally high salinity at Site 2 appeared to have further influenced downgradient transport. The field-measured specific conductivity was ≥ 5 mS/cm for all groundwater samples, with a maximum of 74 mS/cm (i.e., at or above the levels for seawater ~ 50mS/cm). High ionic strength is known to enhance anionic PFAS retention because an abundant supply of multi-valent ions serves to neutralize negatively charged particles and decreases dissolution in groundwater ("salting out"). Apparent K_d values for PFOS and PFHxS (calculated using on paired soil concentrations divided by the groundwater concentrations for samples collected within 0.3 m and assuming equilibrium conditions) showed a positive correlation with specific conductivity using the Spearman's Correlation test, with $p<0.05$ for PFOS (n=5; statistically significant), and p=0.07 for PFHxS (n=6; not statistically significant) (Table S2). These results indicate that elevated salinity is potentially contributing to retardation of these anionic PFAS in groundwater at this site. These partitioning coefficients were generally greater in sands (median = 10.1 L/kg for PFOS; median = 1.03 L/kg for PFHxS) as compared to clays (median = 0.46 L/kg for PFOS; 0.33 L/kg for PFHxS), even though the organic carbon content in samples from clays (median f_{oc} = 0.009) was higher than in samples from sands (median f_{oc} = 0.001). Because the cation exchange capacity in clay samples (median = 15.3 meq per 100 g) was generally higher than in sand samples (median = 2.6 meq per 100 g), this trend suggests that electrostatic forces were a significant factor contributing to the adsorption of anionic PFAS onto sands.

Inter-site comparisons of the estimated groundwater salinity and calculated apparent retardation factors (based on the K_d values described above) showed much higher sorption for Site 2 for PFOA and PFOS compared to Site 1 and Site 3 (Table S3) due to its higher salinity and despite lower organic carbon content. This pattern emphasizes the importance of salting out effects on transport at sites with similar characteristics as Site 2, which is a coastal facility with tidal influences.

Air-water interfacial partitioning

Figure S19 – S27 show the depth-discrete distribution of total PFAS, PFOS, and PFOA at each site. PFAS migration to deeper aquifer intervals was most pronounced at Site 1. The vadose zone is thin at this site (often < 1.5 m bgs) and has been excavated and refilled as part of past remedial activities, such that the retention of PFAS within unsaturated soils due to accumulation at the air-water interface or sorption to soils is likely to be limited. PFAS concentrations in surficial soils were generally lower than those observed in the shallow saturated intervals. Within the saturated zone, PFAS data confirm that concentration of most PFAS increase with depth to about 11 m bgs (Figure S19) with increasing enrichment of more mobile branched isomers (Nickerson et al., 2020). Furthermore, site data confirmed that the former pit is located within a high-recharge groundwater mound with a downward vertical gradient that would promote natural transport between shallow sands and deeper sands, and that the shallow clay layer is relatively thin (< 1 m) within the immediate source area and may not serve as a barrier for vertical transport.

At both Site 2 and Site 3, the highest PFAS concentrations were generally encountered in shallow depth intervals and concentrations decreased with depth (Figure S22, Figure S25). At Site 2, elevated PFAS concentrations at depths greater than 6 m bgs were limited to a few locations with highly permeable soils within the investigated interval where groundwater could be collected. Many locations at Site 2 were dominated by poorly draining, clay-rich soils within the shallow vadose zone. These soils would be expected to have less air-water interfacial retention (due to water logging) and thus less resistance to transfer of AFFF-applied PFAS to the water table.This is consistent with the negative association with clay content and apparent PFAS retention in unsaturated soils that was reported in Anderson et al (2019) based on empirical data from a multi-site survey, as well as the modeling study by Guo et al (2020) where retardation factors in vadose zone clays were predicted to be less than those in sands. However, within the saturated intervals, these clay-rich zones would be less subject to advective flushing, which may limit groundwater transport and promote retention.

At Site 3, both the concentration and the percentage of total PFAS represented by polyfluorinated compounds generally decreased with depth, particularly zwitterionic/cationic PFAS (Figure 3). Given that the percentages of anionic PFAS measured in saturated aquifer solids were generally higher, this is a line of evidence that the charges on PFAS were strongly influencing the partitioning between soil and groundwater. After aggregating all the Site 3 soil data, the median total PFAS concentration (90 ng/g) and median total PFAA concentration (59 ng/g) in unsaturated soils was significantly higher than in saturated soils (19 ng/g Total PFAS, 13 ng/g Total PFAA) from the most impacted intervals (Figure 3) (p=0.02 for two-sided Wilcoxon Rank Sum test). The median total zwitterionic/cationic PFAS concentration in unsaturated soils (24

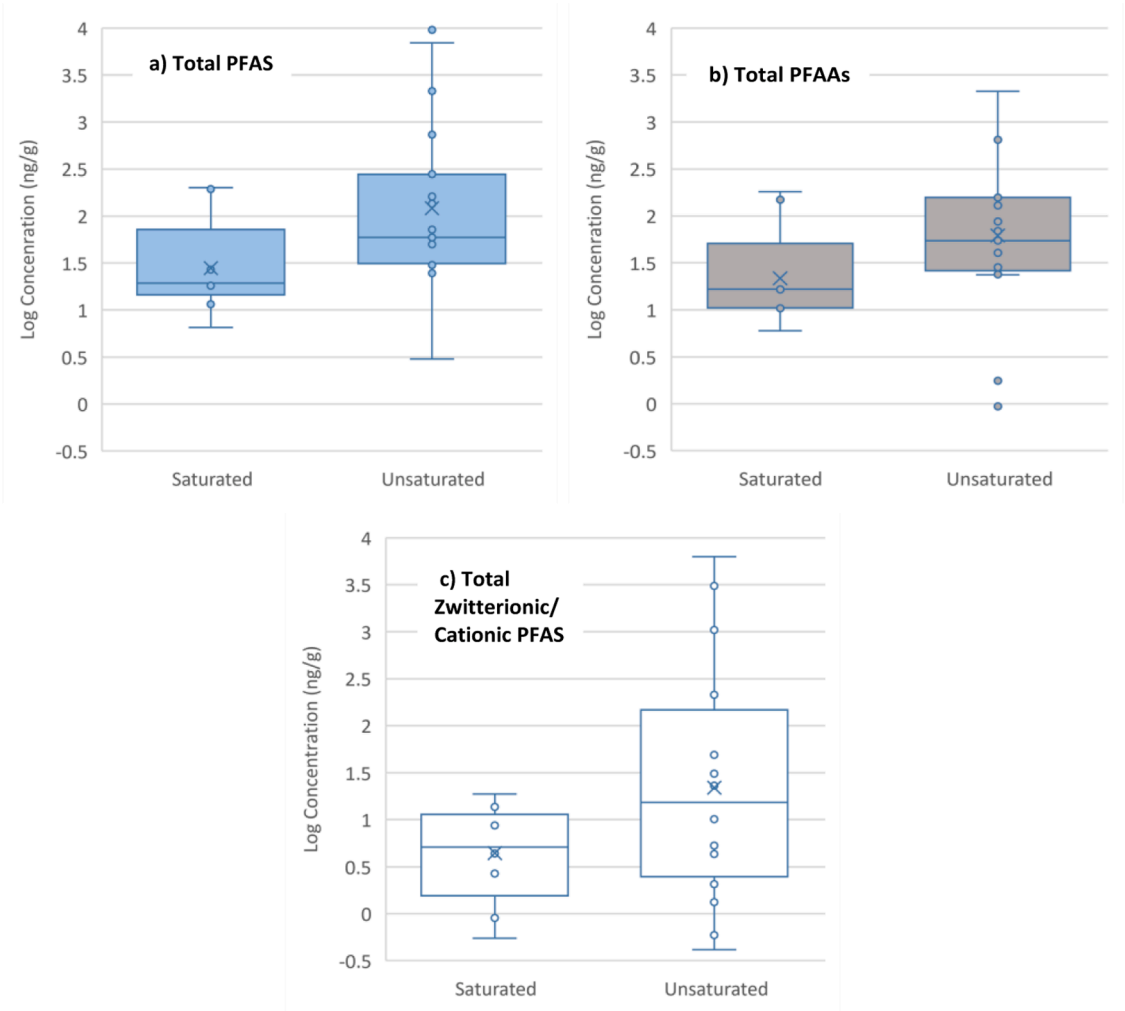

Fig. 3. Site 3 Distribution of Concentrations in Soil Samples from Saturated Zone (samples with max concentration at each location) vs. Unsaturated Zone (all samples from all locations). (a) Total PFAS Concentrations; (b) Total PFAA Concentrations; and (c) Total Zwitterionic/Cationic Concentrations. Data are shown as box and whisker distribution where boxes represent upper and lower quartiles, whiskers represent minimum and maximum values (excluding outliers), and X represents mean value.

ng/g) was also higher than in saturated soils (5.1 ng/g) but did not meet the threshold for statistical significance ($p<0.05$), in part because there were fewer samples with measurable levels of zwitterions/cations to include in the analysis. However, the collective data are consistent with enhanced retention within the unsaturated zone due to air-water interfacial partitioning and solid-phase partitioning processes. Data from unsaturated soil samples indicated that the water content was 17% with a higher fraction of organic carbon (0.01) relative to the site-wide values. However, these unsaturated soils also had a higher cation exchange capacity (median=9.6 meq per 100 g) than saturated soils. which would have contributed to retention of non-anionic PFAS. Several other locations outside of the presumed source area at Site 3 were also characterized by higher concentrations within the shallow unsaturated soils than in the underlying aquifer. It is unlikely that groundwater transport could have plausibly caused this concentration vs. depth pattern. A more plausible scenario is the release of AFFF to the ground surface at these locations, several of which are relatively distant from the presumed source area.

Matrix diffusion

The compartmental modeling reported in Adamson et al. (2020) for Site 1 indicated that retention of PFAS due to diffusion and/or slow advection was significant at that site. Radial flow and vertical gradients observed within the source area likely contributed to migration of PFAS to interfaces between high and low permeability zones. PFAS concentrations were generally higher in shallow clay/silt sublayers relative to adjacent sandier sublayers (Figure S19). Approximately 82% of the total PFAS mass was associated with soils that were classified as lower permeability, including 92% of the precursor mass. These processes can contribute to persistence of precursors within the source area and may limit the rate of conversion to PFAA end products. For example, 93% of the PFAS mass that was in the source area (and 99% of the precursor mass) was found to be associated with lower-permeability soils. In addition, only 6% of the estimated total mass of zwitterionic/cationic PFAS at Site 1 was associated with higher-k intervals, which confirmed that significant retention of zwitterionic and cationic PFAS within lower-permeability zones was occurring at Site 1.

Significant proportions of PFAS mass were also present in lower-permeability compartments at the other two sites. At Site 2, three of the four soil samples with the highest total PFAS concentrations (all from locations L5 and L6) were clay samples. PFAS was present at relatively high concentrations in shallow unsaturated soils throughout the site, and these shallow soils are dominated by low-permeability silts/clays (Figure S22). The only locations where relatively elevated levels of PFOA and PFOS are encountered below 6 m bgs are those where the surficial low-permeability layers are relatively thin and the deeper soil intervals are dominated by sand (L5 and L6). The locations that are dominated by lower-permeability soils (L7, L8, and L9) generally have high specific conductivity levels as well as a higher percentage of precursors. This suggests that polyfluorinated substances that have migrated into these zones (either via diffusion or slow advection) is being retained and subject to slower transformation to PFAAs.

At Site 3, a thin clay and silt-rich layer is present immediately below the sandy surficial soils and above the top of a deeper aquifer. This layer is generally less than 1 m thick but likely slows the rate of vertical advection through the vadose zone (Figure S25). In addition, diffusion of PFAS into this shallow low-permeability soil is likely to promote long-term storage. PFAS were present in samples collected from this clay/silt layer throughout the site, and the concentrations were generally higher than those in the underlying sands. This concentration pattern was distinct within the source area, such as location L3 where shallow soils had both elevated PFAA concentrations but also a high contribution from zwitterionic/cationic precursors (Figure 4). This indicates that PFAS has penetrated the shallow low-permeability soils, presumably from the top, and that further discharge to groundwater may be influenced by slow back diffusion. Confirmation of the importance of matrix diffusion at these sites would require temporal measurements of concentration/mass flux or contaminant transport modeling to help predict plume development.

Biotransformation

Lines of evidence for biotransformation of polyfluorinated precursors to PFAAs was observed at all three sites. For example, the spatial distribution patterns at Site 1 were used to develop a presumptive transformation pathway involving formation of FHxSA via sequential cleavage of the alkyl group at the tertiary and then secondary sulfonamide in a variety of C6 precursors (Nickerson et al., 2020b). Patterns in FHxSA and other suspected degradation intermediates (e.g., fluorotelomer sulfonates, N-dimethyl ammonio propyl-perfluorooctane amide (AmPr-FOAd)) provided further evidence of biotransformation at Site 1. Using a mass balance approach, Adamson et al. (2020) estimated that precursor conversion to PFAAs was occurring at a rate of < 2% annually at this site.

The contribution of precursors to the total PFAS concentration in

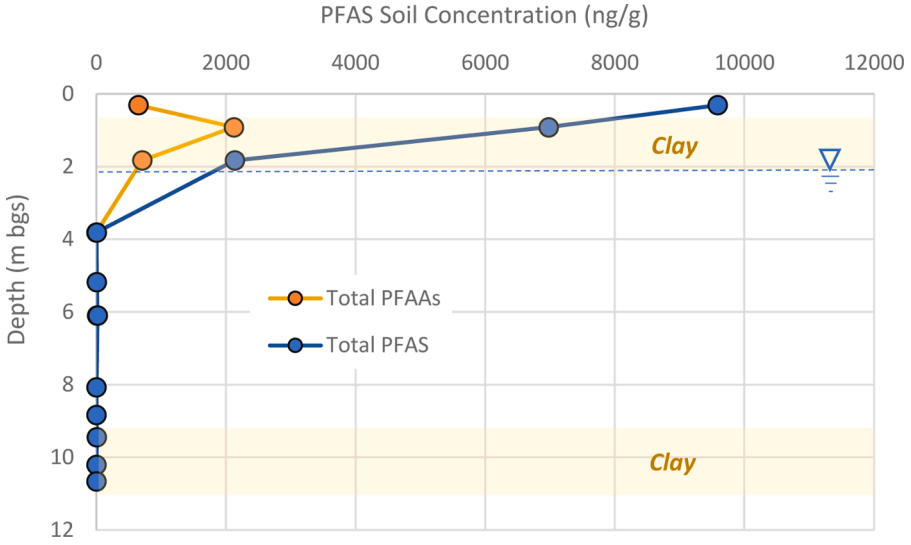

Fig. 4. PFAS Profile with Depth at Location L3 (Source Area) at Site 3.

groundwater samples on a percentage basis generally decreased with distance from the source at Site 1 (Figure S10) and Site 3 (Figure S16), and the concentration of precursors decreased with distance at all three sites. This pattern likely reflects both biotransformation as well as retardation of some precursors (e.g., zwitterionic/cationic species) relative to PFAAs. However, fluorotelomer sulfonates (4:2 FTS, 6:2 FTS, and 8:2 FTS) were among the highest concentrations of all fluorotelomer compounds in both soil and groundwater at all sites. These are relatively mobile, polyfluorinated compounds that are also suspected intermediates in the transformation of other fluorotelomer precursors; they are not considered a major component of AFFF (Field and Seow; 2017; Ruyle et al., 2020), so their high concentrations at these sites are indicative of prior transformation of other fluorotelomer compounds. At Site 2, fluorotelomer sulfonates were present in both soil and groundwater, with the highest concentrations in both matrices generally found near the source within relatively permeable soils where groundwater was collected (location L6; maximum concentration of 6:2 FTS = 230, 000 ng/L in groundwater and 311 ng/g in soil), as well as in both lower and higher permeable soil intervals. Fluorotelomer sulfonates also represented a relatively higher percentage of the total PFAS in several groundwater samples from the location farthest downgradient (L2, L3) of the source area. This pattern is also consistent with biodegradation of polyfluorinated precursor compounds within the plume during transport.

Spatial patterns for other PFAS at Site 2 and Site 3 suggested that biotransformation activity may have been occurring in both the source area and the downgradient PFAS plume. For example, FHxSA was consistently detected in both soil and groundwater at relatively high concentrations at both Site 2 and Site 3 (e.g., 480,000 ng/L in the shallowest groundwater sample and 297 ng/g in the shallowest soil sample from source area location at Site 3). At Site 3, all the presumptive precursors to FHxSA described in the transformation pathway presented in Nickerson et al. (2020b) (i.e., the-perfluorohexane sulfonamido propyl sulfonates) were detected in both soil and groundwater, although they were primarily restricted to the source area. Several other compounds which contain the perfluoroalkyl sulfonamide chain and could therefore be precursors to FHxSA, and ultimately PFHxS (Mejia-Avendaño et al., 2015; Nickerson et al., 2020), were detected at Site 3. For example, zwitterionic TAmPr-N-MeFHxSA and TAmPr-FHxSA were among the highest concentration compounds detected in soil within the source area (at concentrations > 100 ng/g), although they were not detected in groundwater. In groundwater, anionic SPr-FHxSA and zwitterionic CMeAmPr-FHxSA were both detected at greater than 50,000 ng/L at the shallowest sample from source area location L3 (representing approximately 15% of the total PFAS detected in this sample). In general, these C6 precursor compounds were at the highest concentration in the vicinity of the source area and decreased (or were non-detect) in groundwater samples from farther downgradient, further emphasizing that biotransformation was most relevant within the source area. FHxSA groundwater concentrations decreased with distance from the source but were still detected in multiple depths at all downgradient locations, suggesting that some transformation was occurring within the plume.

A summary of relevant fate and transport processes for the three sites are shown in Table 2.

Differentiating other sources

PFAS was present at all locations at all sites, including the background locations that were at least 300 m cross gradient or upgradient of the site-specific locations with highest concentrations. However, the background locations contained relatively low levels in both soil and groundwater relative to source area locations (Figure S28). The number of different precursor compounds detected in some background samples are consistent with not only multiple types of AFFF but also raise the possibility of other PFAS sources. This includes Site 1 where the presence of zwitterionic/cationic PFAS in the source area, as well as the relative absence of zwitterionic/cationic PFAS in background locations in both soil and groundwater, serves as a secondary line of evidence for differentiating between the AFFF source and other diffuse sources. The absence of zwitterionic/cationic species in background locations suggests the PFAS present in these locations is not associated with AFFF releases in the source area.

Site 3 demonstrated the strongest evidence that PFAS in the background locations was unrelated to AFFF use in the source area. For example, PFOS was not detected in the soil at background locations, and only in location B1 in groundwater. In addition, the number of different PFAS detected in some samples are consistent with not only multiple types of AFFF but also raise the possibility of other PFAS sources. In the soil and groundwater samples from location L3 (the presumed source area), a total of 198 different compounds were detected in soil and 75 different compounds were detected in groundwater (Figure S31). This is higher than the number of analytes detected at either of the other two sites included in this study. All background soil samples were dominated by longer-chain PFAAs (e.g., PFPeDA) and/or polyfluorinated, substituted, and unsaturated PFAS, particularly negatively charged other ECF-based derivatives (e.g., unsaturated perfluorooctane sulfonate (UPFOS), hydrido-unsaturated perfluorohexane carboxylate (H-PFHxA) and hydrido-unsaturated perfluoropentane carboxylate (H-PFPeA)), many of which were also found in one or more locations closer to the source area. No compounds unique to the background locations were detected in groundwater samples, but several unique compounds were detected in soil samples (e.g., UPFOS, H-PFPeA). The presence of these compounds suggests that alternative PFAS sources may have contributed to the observed PFAS, although a source cannot be readily identified. No other known or suspected sources of PFAS were reported in site documentation. Compounds that have been proposed to be diagnostic of landfill leachate and/or highly degraded household source, such as shorter chain fluorotelomer intermediates (5:3 FTCA) could not be detected at any location (Lang et al., 2017). However, groundwater samples from the background locations did have a relative abundance of longer-chained fluorotelomer carboxylates. Sulfonamides that are generally not expected to be associated with AFFF (e.g., MeFOSA, EtFOSA, corresponding sulfonamidoacetic acids) were detected sporadically in soil from the source area at trace levels, but not in groundwater or in any background locations. FOSA (a potential degradation product of these compounds as well as precursors present in AFFF) was detected more consistently at multiple locations in both soil and groundwater, and it frequently represented >10% of the total PFAS concentration. Many of the compounds that were unique to the source area and background locations were identified through suspect screening, so care should be taken when using these data for forensic

Table 2
Likely relevant fate and transport processes by site during field characterization.

Site Number	Hydrophobic partitioning	Electrostatic interactions/Salting out	Air-water interfacial partitioning	Matrix diffusion	Bio-transformation
Site 1	Yes	Yes	No[a]	Yes	Yes
Site 2	Yes	Yes [b]	Yes	Yes	Yes
Site 3	Yes	Yes	Yes	Yes	Yes

[a] Shallow vadose zone soils were disturbed due to historic remedial efforts (excavation and low-temperature thermal desorption followed by refilling with treated soil)
[b] Includes salting out effects from high groundwater salinity.

purposes at this and other sites.

Cluster analysis of the Site 3 data provided additional supporting evidence that different PFAS sources were contributing to the observed patterns at background locations. Exploratory analysis with both the soil and groundwater data demonstrated reasonably distinct clustering of source data vs. background locations (Figure S32). When number of variables were reduced to only target analytes, the background location groundwater data forming an even tighter cluster that is distinct from the source area data, which clusters similarly with the groundwater data from the near downgradient and downgradient locations (Figure 5). Note that the source area and plume datasets also cluster with groundwater data from existing monitoring wells at the site (all of which are located near the source) as well as surface water samples from impoundments which are located in the downgradient plume. This suggests that PFAS associated with AFFF releases in the former AFFF storage/transfer area are the source of PFAS detected in the plume, even after accounting for shifts in composition during transport. These results also suggest that runoff of PFAS from surficial soils (which exhibit high PFAS concentration relative to deeper soils at this site) is likely contributing to PFAS detected in the surface water impoundments. This distinct clustering of the background location data becomes even more apparent when only the data from source area location L3 and background location B1 and B2 were included (Figure 5, bottom panel). The confidence intervals for the background data do not overlap with the confidence interval for the source area location.

Conclusion

By quantifying a large suite of PFAS from AFFF release areas along transport pathways, the field study suggested the relevance of expected PFAS fate and transport processes on PFAS distribution across multiple sites. Of those processes that were examined, only one (air-water interfacial partitioning) at a single site (Site 1) was not supported by the field data. In this specific case, disturbance of site soils as part of historic remedial efforts likely redistributed PFAS mass and prevented any clear indication of vadose zone retention. In all other cases, there were lines of evidence that multiple processes were active; many of these processes are physical-chemical and are expected to occur in most natural settings. In addition, site-specific properties were shown to influence retention. For example, high groundwater salinity enhanced apparent PFAS retardation at one site, which has implications for PFAS plume migration in coastal areas. While significant PFAS transport beyond the source area was observed at all three sites, attenuation of PFAS concentrations with distance from these AFFF-based sources was also apparent due to processes that retard transport and/or transform PFAS present in the source material.

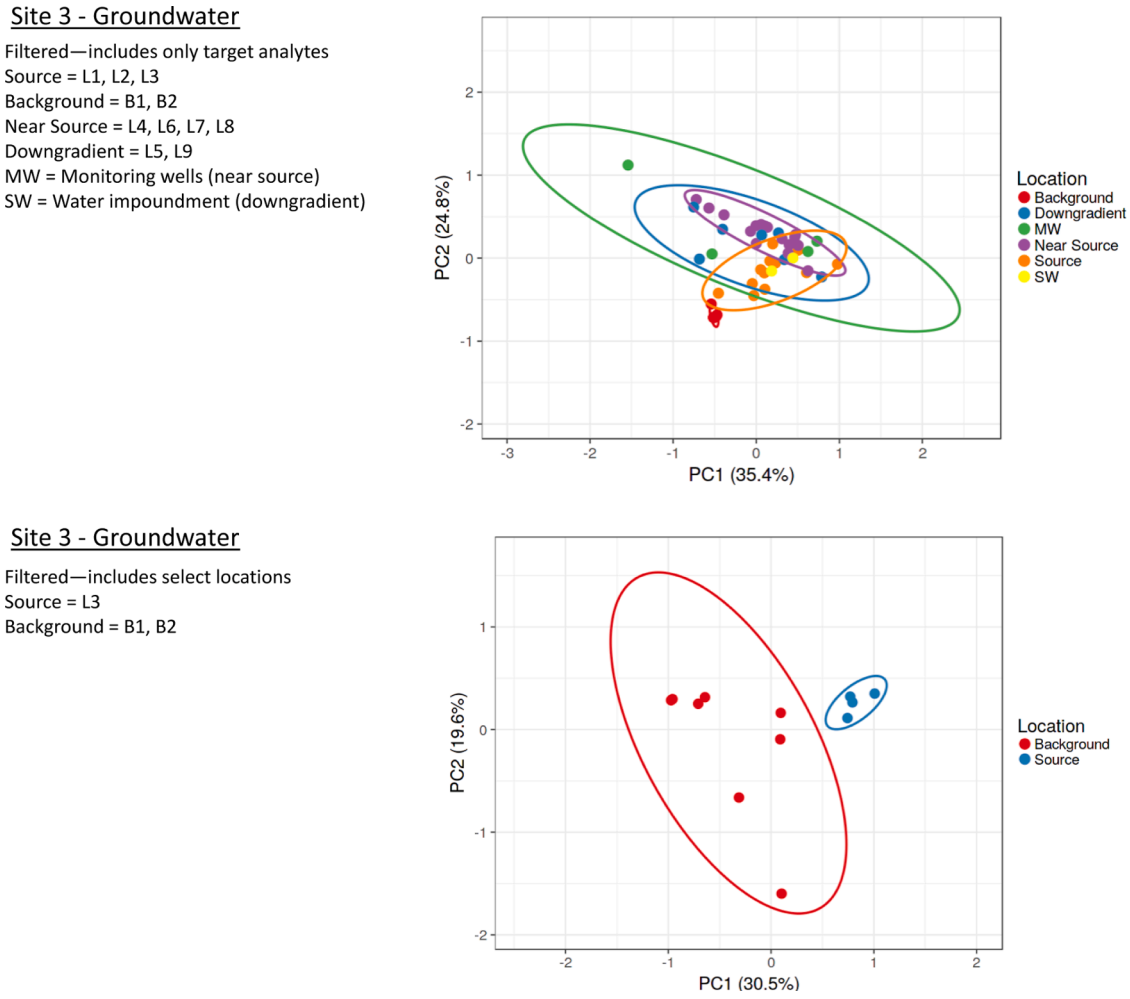

Fig. 5. Principal Component Analysis for Groundwater Target Analyte Data from All Locations (Top Panel) and Groundwater Target and Non-Target Data from Select Locations (Bottom Panel) from Site 3. Analyses performed on transformed data where constituent concentrations were converted to percentage of total PFAS concentration. Transformed data were entered into ClustVis (http://biit.cs.ut.ee/clustvis/). Clustering was performed using Euclidean distances, and Ward's Method was selected for linking clusters. Detailed methods associated with this tool for cluster analysis are described in Metsalu and Vilo, 2015.

Author statement

David Adamson: Writing – Original draft preparation, Conceptualization, Methodology, Formal Analysis, Visualization

Poonam Kulkarni: Conceptualization, Methodology, Formal Analysis, Investigation, Writing – Reviewing and Editing

Anastasia Nickerson: Investigation, Formal Analysis, Writing – Reviewing and Editing

Christopher Higgins: Conceptualization, Methodology, Writing – Reviewing and Editing

Jennifer Field: Conceptualization, Methodology, Writing – Reviewing and Editing

Trever Schwichtenberg: Investigation, Formal Analysis, Writing – Reviewing and Editing

Charles Newell: Conceptualization, Methodology, Formal Analysis, Writing – Reviewing and Editing

John Kornuc: Methodology, Writing - Reviewing and Editing, Supervision, Project Management

Supporting information

Details regarding PFAS site characterization data. This information is available free of charge via the Internet at http://pubs.acs.org.

Declaration of Competing Interest

The authors declare that they have no known competing financial interests or personal relationships that could have appeared to influence the work reported in this paper.

Acknowledgements

Technical support was provided by Clayton Sorensen, Wade (Ben) Smith, Kenneth Walker, Blossom Nzeribe, Brian Strasert, Dylan Hart, Josh Voss, Victoria Boyd, Hassan Javed, Barbara Carrera, Christ Niamike, Beatrice Li, Jessica Alanis, Robin McDonald, and Justin Long (GSI Environmental Inc.). We thank the base personnel for supporting the demonstration. Additional consultation was provided by Pati Moreno (Naval Facilities Engineering and Expeditionary Warfare Center) and Graham Peaslee (University of Notre Dame). This project was supported by Environmental Security Technology Certification Program (project ER-201633) and the Navy Environmental Sustainability Development to Integration Program.

Supplementary materials

Supplementary material associated with this article can be found, in the online version, at doi:10.1016/j.envadv.2022.100167.

References

Adamson, D.T., Nickerson, A., Kulkarni, P.R., Higgins, C.P., Popovic, J., Field, J., Rodowa, A., Newell, C., DeBlanc, P., Kornuc, J.J., 2020. Mass-Based, Field-Scale Demonstration of PFAS Retention within AFFF-Associated Source Areas. Environ. Sci. Technol. 54 (24), 15768–15777.

Anderson, R.H., Long, G.C., Porter, R.C., Anderson, J.K., 2016. Occurrence of select perfluoroalkyl substances at US Air Force aqueous film-forming foam release sites other than fire-training areas: Field-validation of critical fate and transport properties. Chemosphere 150, 678–685.

Anderson, R.A, Adamson, D.T., Stroo, H.F, 2019. Partitioning of Poly- and Perfluoroalkyl Substances from Soil to Groundwater within Aqueous Film-Forming Foam Source Zones. J. Contam. Hydrol. 220, 59–65, 2019.

Baduel, C., Mueller, J.F., Rotander, A., Corfield, J., Gomez-Ramos, M.J., 2017. Discovery of Novel Per- and Polyfluoroalkyl Substances (PFASs) at a Fire Fighting Training Ground and Preliminary Investigation of Their Fate and Mobility. Chemosphere 185, 1030–1038.

Barzen-Hanson, K.A., Davis, S.E., Kleber, M., Field, J.A., 2017. Sorption of Fluorotelomer Sulfonates, Fluorotelomer Sulfonamido Betaines, and a Fluorotelomer Sulfonamido Amine in National Foam Aqueous Film-Forming Foam to Soil. Environ. Sci. Technol. 51 (21), 12394–12404.

Benskin, J.P., Yeung, L.W.Y., Yamashita, N., Taniyasu, S., Lam, P.K.S., Martin, J.W., 2010. Perfluorinated Acid Isomer Profiling in Water and Quantitative Assessment of Manufacturing Source. Environ. Sci. Technol. 44 (23), 9049–9054.

Brusseau, M.L., Anderson, R.H., Guo, B., 2020. PFAS concentrations in soils: Background levels versus contaminated sites. Sci. Total Environ. 740, 140017.

Costanza, J., Arshadi, M., Abriola, L.M., Pennell, K.D., 2019. Accumulation of PFOA and PFOS at the air–water interface. Environ. Sci. Tech. Lett. 6 (8), 487–491.

Costanza, J., Abriola, L.M., Pennell, K.D., 2020. Aqueous film-forming foams exhibit greater interfacial activity than PFOA, PFOS, or FOSA. Environ. Sci. Technol. 54 (21), 13590–13597.

Dauchy, X., Boiteux, V., Colin, A., Hémard, J., Bach, C., Rosin, C., Munoz, J.F., 2019. Deep Seepage of Per- and Polyfluoroalkyl Substances through the Soil of a Firefighter Training Site and Subsequent Groundwater Contamination. Chemosphere 214, 729–737.

Du, Z., Deng, S., Bei, Y., Huang, Q., Wang, B., Huang, J., Yu, G., 2014. Adsorption behavior and mechanism of perfluorinated compounds on various adsorbents—A review. J. Hazard. Mater. 274, 443–454.

Field, J.A., Seow, J., 2017. Properties, occurrence, and fate of fluorotelomer sulfonates. Crit. Rev. Environ. Sci. Technol. 47 (8), 643–691.

Guelfo, J.L., Higgins, C.P., 2013. Subsurface transport potential of perfluoroalkyl acids at aqueous film-forming foam (AFFF)-impacted sites. Environ. Sci. Technol. 47 (9), 4164–4171.

Guelfo, J.L., Adamson, D.T., 2018. Evaluation of a national data set for insights into sources, composition, and concentrations of per-and polyfluoroalkyl substances (PFASs) in US drinking water. Environ. Pollut. 236, 505–513.

Guelfo, Jennifer L., Korzeniowski, Stephen, Mills, Marc A., Anderson, Janet, Anderson, Richard H., Arblaster, Jennifer A., Conder, Jason M., et al., 2021. Environmental Sources, Chemistry, Fate and Transport of Per-and Polyfluoroalkyl Substances: State of the Science, Key Knowledge Gaps, and Recommendations Presented at the August 2019 SETAC Focus Topic Meeting. Environ. Toxicol. Chem.

Guo, B., Zeng, J., Brusseau, M.L., 2020. A Mathematical Model for the Release, Transport, and Retention of Per-and Polyfluoroalkyl Substances (PFAS) in the Vadose Zone. Water Resour. Res. 56 (2) p.e2019WR026667.

Hatton, J., Holton, C., DiGuiseppi, B., 2018. Occurrence and behavior of per-and polyfluoroalkyl substances from aqueous film-forming foam in groundwater systems. Remed. J. 28 (2), 89–99.

Higgins, C.P., Luthy, R.G., 2006. Modeling sorption of anionic surfactants onto sediment materials: an a priori approach for perfluoroalkyl surfactants and linear alkylbenzene sulfonates. Environ. Sci. Technol. 41 (9), 3254–3261. https://doi.org/10.1021/es062449j.

Høisæter, Å., Pfaff, A., Breedveld, G.D., 2019. Leaching and Transport of PFAS from Aqueous Film-Forming Foam (AFFF) in the Unsaturated Soil at a Firefighting Training Facility under Cold Climatic Conditions. J. Contam. Hydrol. 222, 112–122.

Lang, J.R., Allred, B.M., Field, J.A., Levis, J.W., Barlaz, M.A., 2017. National estimate of per-and polyfluoroalkyl substance (PFAS) release to US municipal landfill leachate. Environ. Sci. Technol. 51 (4), 2197–2205.

Leeson, A., Thompson, T., Stroo, H.F., Anderson, R.H., Speicher, J., Mills, M.A., Willey, J., Coyle, C., Ghosh, R., Lebrón, C., Patton, C., 2021. Identifying and managing aqueous film-forming foam-derived per-and polyfluoroalkyl substances in the environment. Environ. Toxicol. Chem. 40 (1), 24–36.

Liu, Y., D'Agostino, L.A., Qu, G., Jiang, G., Martin, J.W., 2019. High-resolution mass spectrometry (HRMS) methods for nontarget discovery and characterization of poly-and per-fluoroalkyl substances (PFASs) in environmental and human samples. TrAC Trends Anal. Chem. 121, 115420.

Lyu, Y., Brusseau, M.L., 2020. The influence of solution chemistry on air-water interfacial adsorption and transport of PFOA in unsaturated porous media. Sci. Total Environ. 713, 136744.

McGuire, M.E., Schaefer, C., Richards, T., Backe, W.J., Field, J.A., Houtz, E., Sedlak, D.L., Guelfo, J.L., Wunsch, A., Higgins, C.P, 2014. Evidence of Remediation-Induced Alteration of Subsurface Poly- and Perfluoroalkyl Substance Distribution at a Former Firefighter Training Area. Environ. Sci. Technol. 48 (12), 6644–6652.

Mejia-Avendaño, S., Zhi, Y., Yan, B., Liu, J., 2020. Sorption of polyfluoroalkyl surfactants on surface soils: Effect of molecular structures, soil properties, and solution chemistry. Environ. Sci. Technol. 54 (3), 1513–1521.

Munoz, G., Budzinski, H., Labadie, P., 2017. Influence of Environmental Factors on the Fate of Legacy and Emerging Per- and Polyfluoroalkyl Substances along the Salinity/Turbidity Gradient of a Macrotidal Estuary. Environ. Sci. Technol. 51, 12347–12357.

Newell, C.J., Adamson, D.T., Kulkarni, P.R., Nzeribe, B.N., Connor, J.A., Popovic, J., Stroo, H.F., 2021. Monitored natural attenuation to manage PFAS impacts to groundwater. Part 1: Scientific basis. Ground Water Monitoring & Remediation. Accepted.

Nguyen, T.M.H., Bräunig, J., Thompson, K., Thompson, J., Kabiri, S., Navarro, D.A., Kookana, R.S., Grimison, C., Barnes, C.M., Higgins, C.P., McLaughlin, M.J., 2020. Influences of chemical properties, soil properties, and solution pH on soil–water partitioning coefficients of per-and polyfluoroalkyl substances (PFASs). Environ. Sci. Technol. 54 (24), 15883–15892.

Nickerson, A., Maizel, A.C., Kulkarni, P.R., Adamson, D.T., Kornuc, J.J., Higgins, C.P., 2020a. Enhanced Extraction of AFFF-Associated PFASs from Source Zone Soils. Environ. Sci. Technol. 54, 4952–4962.

Nickerson, A., Rodowa, A.E., Adamson, D.T., Field, J.A., Kulkarni, P.R., Kornuc, J.J., Higgins, C.P., 2020b. Spatial trends of anionic, zwitterionic, and cationic PFASs at an AFFF-impacted site. Environ. Sci. Technol. 55 (1), 313–323.

Quinnan, J., Rossi, M., Curry, P., Lupo, M., Miller, M., Korb, H., Orth, C., Hasbrouck, K., 2021. Application of PFAS-mobile lab to support adaptive characterization and flux-based conceptual site models at AFFF releases. Remed. J.

Rankin, K., Mabury, S.A., Jenkins, T.M., Washington, J.W., 2016. A North American and global survey of perfluoroalkyl substances in surface soils: Distribution patterns and mode of occurrence. Chemosphere 161, 333–341.

Ruyle, B.J., Thackray, C.P., McCord, J.P., Strynar, M.J., Mauge-Lewis, K.A., Fenton, S.E., Sunderland, E.M., 2020. Reconstructing the Composition of Per-and Polyfluoroalkyl Substances in Contemporary Aqueous Film-Forming Foams. Environ. Sci. Tech. Lett. 8 (1), 59–65.

Schaefer, C.E., Culina, V., Nguyen, D., Field, J.A., 2019. Update of Poly- and Perfluorinated Substances at the Air-Water Interface. Environ. Sci. Technol. 53 (21), 12442–12448.

Schwichtenberg, T., Bogdan, D., Carignan, C.C., Reardon, P., Rewerts, J., Wanzek, T., Field, J.A., 2020. PFAS and dissolved organic carbon enrichment in surface water foams on a northern US freshwater lake. Environ. Sci. Technol. 54 (22), 14455–14464.

Sharifan, H., Bagheri, M., Wang, D., Burken, J.G., Higgins, C.P., Liang, Y., Liu, J., Schaefer, C.E., Blotevogel, J., 2021. Fate and transport of per-and polyfluoroalkyl substances (PFASs) in the vadose zone. Sci. Total Environ., 145427

Silva, J.A., Martin, W.A., McCray, J.E., 2021. Air-water interfacial adsorption coefficients for PFAS when present as a multi-component mixture. J. Contam. Hydrol. 236, 103731.

Sörengård, Mattias, Ahrens, Lutz, Alygizakis, Nikiforos, Jensen, Pernille Erland, Gago-Ferrero, Pablo, 2020. Non-target and suspect screening strategies for electrodialytic soil remediation evaluation: Assessing changes in the molecular fingerprints and per- and polyfluoroalkyl substances (PFASs). J. Environ. Chem. Eng. 8 (6), 104437.

Wang, S., Ma, L., Chen, C., Li, Y., Wu, Y., Liu, Y., Dou, Z., Yamazaki, E., Yamashita, N., Lin, B.L., Wang, X., 2020. Occurrence and partitioning behavior of per- and polyfluoroalkyl substances (PFASs) in water and sediment from the Jiulong Estuary-Xiamen Bay, China. Chemosphere 238, 124578.

Weber, A.K., Barber, L.B., Leblanc, D.R., Sunderland, E.M., Vecitis, C.D., 2017. Geochemical and Hydrologic Factors Controlling Subsurface Transport of Poly- and Perfluoroalkyl Substances, Cape Cod, Massachusetts. Environ. Sci. Technol. 51, 4269–4279.

Xiao, F., Jin, B., Golovko, S.A., Golovko, M.Y., Xing, B., 2019. Sorption and Desorption Mechanisms of Cationic and Zwitterionic Per-and Polyfluoroalkyl Substances in Natural Soils: Thermodynamics and Hysteresis. Environ. Sci. Technol. 53 (20), 11818–11827.